How to cite: *Angew. Chem. Int. Ed.* **2020**, *59*, 16371 – 16375
International Edition: doi.org/10.1002/anie.202004618
German Edition: doi.org/10.1002/ange.202004618

CO_2 Methanation

CO_2 Methanation via Amino Alcohol Relay Molecules Employing a Ruthenium Nanoparticle/Metal Organic Framework Catalyst

Xinjiang Cui, Serhii Shyshkanov, Tu N. Nguyen, Arunraj Chidambaram, Zhaofu Fei, Kyriakos C. Stylianou, and Paul J. Dyson**

Abstract: *Methanation of carbon dioxide (CO_2) is attractive within the context of a renewable energy refinery. Herein, we report an indirect methanation method that harnesses amino alcohols as relay molecules in combination with a catalyst comprising ruthenium nanoparticles (NPs) immobilized on a Lewis acidic and robust metal–organic framework (MOF). The Ru NPs are well dispersed on the surface of the MOF crystals and have a narrow size distribution. The catalyst efficiently transforms amino alcohols to oxazolidinones (upon reaction with CO_2) and then to methane (upon reaction with hydrogen), simultaneously regenerating the amino alcohol relay molecule. This protocol provides a sustainable, indirect way for CO_2 methanation as the process can be repeated multiple times.*

The development of new approaches to utilize CO_2 remains important due to continued anthropogenic emissions (around 37.1 billion tons in 2018) resulting in global warming. The catalytic transformation of CO_2 into useful hydrocarbon fuels is a key process in C1 chemistry,[1–5] with methanation being a particularly appealing catalytic process. Catalysts based on noble metals (Pt, Ru, Pd, Rh) supported on metal oxides (CeO_2, TiO_2, Al_2O_3, SiO_2, ZrO_2, MgO) have been extensively investigated for direct CO_2 methanation.[6–13] Despite recent progress, due to the requirement of an eight-electron process for the direct reduction of CO_2 to methane, forcing conditions are required to overcome the kinetic limitations. At the same time, CO_2 methanation is an exothermic reaction; hence, high temperatures deteriorate the overall performance of the reaction and lead to the formation of side-products, such as CO. Thus, the development of catalytic systems operating at comparatively low temperatures is crucial for improving the efficiency of the process and avoid the formation of side-products.[12]

Recently, we explored an indirect method for CO_2 methanation where organic carbonates were used as relay molecules due to the facile synthesis of carbonates from CO_2 and epoxides.[14] Methane is selectively generated after hydrogenation of the organic carbonates under mild conditions, simultaneously producing diols. Although the corresponding diols are more valuable than the epoxide precursors, they are not easily transformed into organic carbonates making the process complicated[15] and a superior relay molecule is needed.

Industrially, the most common methods used for CO_2 capture are based on chemical CO_2 absorption using amines or amino alcohols as agents producing carbamates.[16–18] Using such methods, CO_2 can be separated and stored.[19–24] Moreover, the CO_2 may be liberated from the carbamates by thermal treatment and the produced amine is regenerated. Recently, Milstein reported the efficient hydrogenation of oxazolidinones into the corresponding amino ethanol and methanol using Ru-based PNN pincer catalysts.[19] However, to the best of our knowledge, the indirect reduction of CO_2 via carbamates to methane has not been reported. Herein, we describe a catalyst for this process comprising Ru NPs immobilized on an intrinsically Lewis acidic MOF (Scheme 1).

In previous studies, MOF materials were used as efficient catalysts for different reactions,[25–29] including CO_2 capture and conversion.[30,31] Recently, we synthesized a MOF, named SION-105, based on Eu^{III} and a tricarboxylate ligand with Lewis acidic boron centers, which functions as a heteroge-

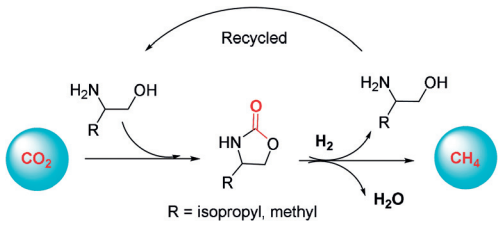

Scheme 1. Indirect pathway for CO_2 methanation via amino alcohols employed as relay molecules.

[*] Dr. X. Cui, S. Shyshkanov, Dr. Z. Fei, Prof. P. J. Dyson
Institute of Chemical Sciences and Engineering
École Polytechnique Fédérale de Lausanne (EPFL)
1015 Lausanne (Switzerland)
E-mail: paul.dyson@epfl.ch
Dr. T. N. Nguyen, A. Chidambaram, Prof. K. C. Stylianou
Institute of Chemical Sciences and Engineering
École Polytechnique Fédérale de Lausanne (EPFL Valais)
Rue de l'Industrie 17, 1951 Sion (Switzerland)
Prof. K. C. Stylianou
Department of Chemistry, Oregon State University
53 Gilbert Hall, Corvallis, OR 97331-4003 (USA)
E-mail: kyriakos.stylianou@oregonstate.edu
Dr. T. N. Nguyen
Helen Scientific Research and Technological Development Co., Ltd.
Ho Chi Minh City (Vietnam)
Supporting information and the ORCID identification number(s) for the author(s) of this article can be found under: https://doi.org/10.1002/anie.202004618.

neous catalyst for the synthesis of benzimidazoles, using CO_2 as a C1 building block.[32] The three-coordinate B center of the (tris(*p*-carboxylic acid) tridurylborane, H_3tctb) ligand of SION-105 is protected by bulky duryl groups, precluding irreversible binding with Lewis bases, such as water, thus, providing exceptional stability and moisture tolerance. At the same time, B remains accessible for the activation of CO_2 as a Lewis acid site.[32] The Eu^{III} centers might also act as Lewis acidic sites enhancing the catalytic activity.[33] The catalyst was prepared from SION-105 via an impregnation–reduction process using $RuCl_3$ as the NP precursor. The Ru^{III} ions anchor within the MOF matrix of SION-105 and following reduction with H_2, Ru NPs anchor to the surface of SION-105, forming the catalyst termed Ru/SION-105 (see the Supporting Information for full details).

Transmission electron microscopy (TEM) and high-angle annular dark-field (HADDF) imaging were used to characterize the Ru/SION-105 catalyst (Figures 1 and S1). As shown in Figure 1 a, the Ru NPs are uniformly dispersed and have a narrow size distribution of 1.5–3 nm with an average diameter of 2.16 nm, suggesting the formation of the NPs was controlled on the surface of the MOF support (Figure 1 f). The high-resolution TEM (HRTEM) image shows a typical Ru NP with an interplanar spacing of 2.0 Å,[34,35] corresponding to a face-centered cubic (fcc) lattice structure with a (101) surface. HADDF-STEM was used to further investigate the size range and elemental distribution of the Ru NPs (Figure 1 c,d), and energy-dispersive X-ray (EDX) spectroscopy confirms the presence of Ru, Eu, and O (Figure 1 e). Ru NPs supported on carbon or Al_2O_3 supports are considerably larger and more aggregated in the case of the latter support (see Figures S1 and S2). It is known the porous structure of MOFs with functionalized surface provide a suitable environment for the growth of NPs leading to the formation of NPs with smaller sizes and more surface metal sites.[36–38] Indeed, TEM characterization revealed that the Ru NPs formed on Ru/SION-105 are smaller than those on Ru/C and Ru/Al_2O_3, presumably leading to the higher catalytic activity observed for Ru/SION-105 (Table 1). Moreover, compared to the absorbed oxygen or lattice oxygen on the surface of C and Al_2O_3, the oxygen in the MOF matrix is comparatively stable and does not appear be involved in reaction leading to higher a selectivity for CH_4.

The electronic structure of the Ru NPs immobilized on SION-105 was probed with X-ray photoelectron spectroscopy (XPS). In the overall XPS survey, due to the overlap of peaks around 285 eV corresponding to C 1s and Ru 3d, assignment is hampered (Figure S4), and hence Ru 3p was used for the analysis. Figure 2 b presents the Ru $3p_{3/2}$ spectrum of the Ru/SION-105 catalyst. The binding energy (BE) of 462.4 eV was attributed to metallic Ru, whereas the low-intensity peak at 463.7 eV[39] may be related to the formation of Ru–O linkages

Table 1: Optimization of the hydrogenation of 4-isopropyl-2-oxazolidinone (**1 a**).[a]

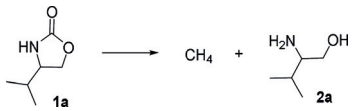

Entry	Catalyst	*t* [h]	Conv. [%]	Yield of **2 a** [%][b]	CH_4	CO_2	CO
1	Ru/SION-105	6	36	31	90	9	1
2	Ru/SION-105	9	50	45	98	1	1
3	Ru/SION-105	12	63	54	98	1	1
4	Ru/SION-105	15	81	66	98	1	1
5	Ru/SION-105	18	92	69	98	1	1
6	Ru/SION-105	20	99	71	98	1	1
7	Ru/C	20	56	39	70	29	1
8	Ru/Al_2O_3	20	49	31	56	42	2
9	Pd/C	20	15	8	48	39	13
10	Rh/C	20	17	11	51	41	8

[a] Reaction conditions: catalyst (0.3 mol% of metal), **1 a** (0.5 mmol), solvent (0.5 mL), H_2 (70 bar), 205 °C. The gas phase was analyzed by GC-TCD. [b] Conversion was estimated by ^{1}H NMR spectroscopy with diphenylmethanol used as an internal standard.

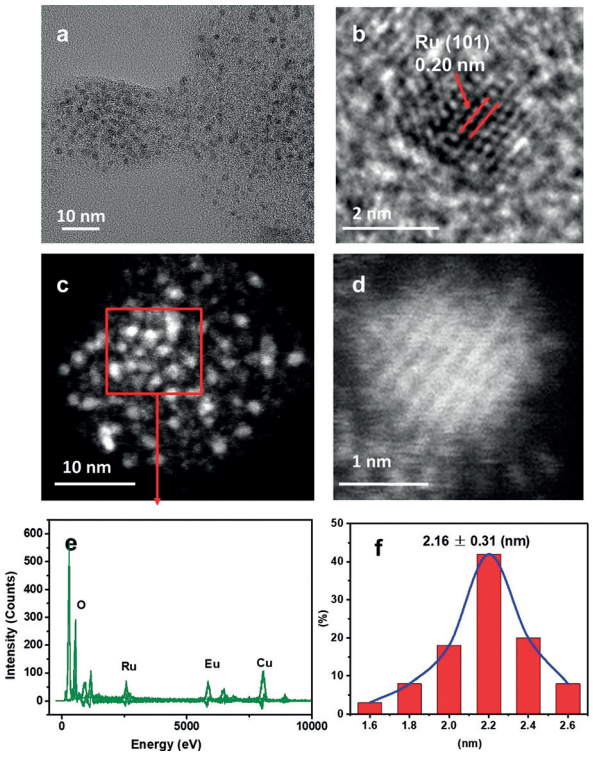

Figure 1. Characterization of the Ru/SION-105 catalyst: a) Bright field TEM image; b) HR-TEM image; c, d) HAADF-STEM images; e) TEM-EDX; f) size distribution based on 80 NPs.

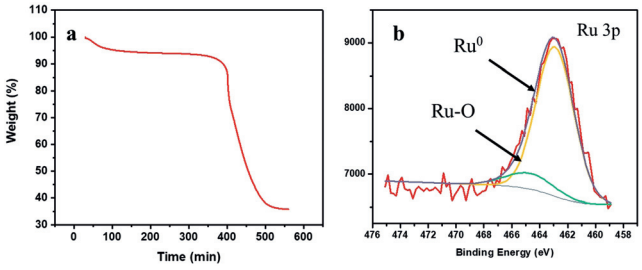

Figure 2. a) TGA curve of the Ru/SION-105 catalyst and b) XPS spectrum for Ru 3p of Ru/SION-105.

between the edge of the Ru NPs and the carboxyl groups of the MOF. This interaction may be relevant in controlling the size and dispersion of the Ru NPs on the surface of SION-105.[40] Moreover, XPS analysis revealed more oxidized Ru species are present in Ru/C and Ru/Al_2O_3 (Figure S5), which probably decrease their catalytic performance. Compared to SION-105,[32] the powder X-ray diffraction (XRD) profile of Ru/SION-105 displayed no additional peaks attributable to very small Ru NPs (Figure S6).

Thermogravimetric analysis (TGA) was used to examine the structural stability of the SION-105 support and the Ru/SION-105 catalysts. As shown in Figure 2a, the Ru/SION-105 catalyst displayed two weight loss steps. The weight loss below 100 °C corresponds to the desorption of encapsulated solvent/water. As the temperature is increased, the catalyst remains stable up to 360 °C, which is comparable to the decomposition temperature of SION-105 (Figure S7), showing that the immobilized Ru NPs do not affect the thermal stability of SION-105. At around 400 °C a sharp weight loss is observed, initiated by the decarboxylation of organic linkers.[41] Nevertheless, the decomposition temperature is well above 300 °C, which is more than sufficient for the catalyst to endure the reaction temperatures required for methanation. CO_2 isotherms on SION-105 and Ru/SION-105 collected at 195 K and 1 bar revealed that the total CO_2 uptake of both materials is comparable (Figure S8). This suggests that the presence of Ru NPs on SION-105 does not affect the sorption behavior of the material.

Fluorescence spectroscopy was used to evaluate the effect of the Lewis acidic Eu^{III} centers in Ru/SION-105. Irradiation of Ru/SION-105 with UV ($\lambda_{exc} = 365$ nm) in THF solution led to a bright-red Eu^{III}-based emission centered at 618 nm (Figure S9). The addition of the substrate, 4-isopropyl-2-oxazolidinone (**1a**, see below), in THF at concentrations of 0.2 and 0.4 mmol L^{-1} resulted in a luminescence quenching response indicating an interaction of **1a** with the Eu^{III} ions. Considering the electronic configuration of Eu^{III} and its large ionic radius (94.7 pm), high coordination numbers are possible.[42,43] It is therefore likely that the Eu^{III} ions can expand their coordination sphere, possible forming Eu^{III}–O bonds with the C=O group in **1a**, resulting in fluorescence quenching and activating the C=O bond. The observed quenching might also be due to the formation of H-bonding interactions between **1a** and coordinated water molecules to Eu.

To evaluate and optimize the reaction conditions for the indirect hydrogenation of CO_2, 4-isopropyl-2-oxazolidinone (**1a**) was chosen as a substrate (Table 1). After reaction at 205 °C for 6 h using 2-pyrrolidinone as solvent, 36% conversion was observed with 31% yield of valinol (**2a**) formed as the main liquid product (determined using ^{1}H NMR spectroscopy). The gaseous products were analyzed by gas chromatography–thermal conductivity detection (GC-TCD) and methane was the main product (90% selectivity) with traces of CO (1%) and CO_2 (9%) detected (Table 1, entry 1). The formation of CO_2 is presumably due to the hydrolysis of **1a** in the presence of water in the solution or the water produced during the reaction. As expected, the conversion of **1a** increases as the reaction time is prolonged and full conversion was observed after 20 h (Table 1, entries 2–6, Table S2). Interestingly, CO_2 produced at the earlier stage of the reaction is converted to methane after prolonged reaction. Note that methane was not detected under the same reaction conditions in the absence of **1a**, indicating that CO_2 is derived from **1a** and the 2-pyrrolidinone solvent is inert and not involved in the reaction (Table S3).

To obtain a high yield of **2a**, the effect of various solvents with different polarities, such as dodecane and ethylene glycol, on the catalytic performance of Ru/SION-105 were studied (Table S3). Compared to 2-pyrrolidinone, dodecane resulted in a lower conversion of **1a** (34%) and a yield of **2a** of 21%, presumably due to mass transfer limitations based on the poor solubility of **1a** and H_2 in dodecane.[44] As expected, the catalytic performance of Ru/SION-105 was improved in ethylene glycol, with a conversion of 81% and a yield of **2a** of 57%, where hydrogen bonding between **1a** and ethylene glycol could help to activate the substrate.[45] However, the hydrogenolysis of ethylene glycol occurred during the hydrogenation, leading to the formation of isopropanol and water.[14] The in situ formed water leads to hydrolysis of **1a** lowering the selectivity to methane (87%) and increasing the CO_2 content to 12%. Consequently, 2-pyrrolidinone was used as the optimal solvent for subsequent studies.

For comparison, Ru/C and Ru/Al_2O_3 catalysts were investigated as catalysts for this reaction, which led to 56% and 49% conversion of **1a** and lower yields of the amino alcohol **2a** and methane (Table 1, entries 7 and 8). Moreover, other precious metal catalysts were also investigated, which also resulted in lower conversions and yields of **1a** (Table 1, entries 9 and 10). Moreover, the amino alcohol product **2a** is further converted into 2-propanol and propane due to the hydrogenolysis/hydrolysis, lowering the yield of **2a**.

The influence of reaction temperature on the catalytic performance of Ru/SION-105 was studied in the range of 165–205 °C (Figure 3a). Under 70 bar of hydrogen pressure after 20 h, the conversion of **1a** increases from 12% at 165 °C to 99% at 205 °C with methane formed with a selectivity of 99%. The yield of **2a** increases to 71% (Figure S10). Note that the amino alcohol can be obtained with high selectivity at lower reaction temperatures, although the conversion is low. The effect of H_2 pressure on the reaction was also studied (Figure 3b), with the conversion dramatically affected. Only 13% conversion was obtained under 40 bar of hydrogen, but increasing the pressure to 70 bar leads to full conversion at 205 °C after 20 h. The selectivity to methane in all cases is > 99% (Figure S11).

The stability and recyclability of the Ru/SION-105 catalyst were evaluated (Figure S12), with only a slight decrease in catalytic activity and selectivity observed after five successive runs. TEM analysis of the used catalyst reveals that the size of the Ru NPs increased to 3.0 nm after five cycles, rationalizing the decrease in catalytic activity (Figure S3. XRD analysis of the used catalyst shows that it is essentially unchanged relative to the pristine catalyst (Figure S6). Furthermore, the XPS spectrum of the recycled catalyst remains similar to that of the pristine catalyst (Figure S13) and Ru leaching was not observed (Table S1).

The reaction of 3-methyl-2-oxazolidinone (**1b**) was examined in 2-pyrrolidinone using the Ru/SION-105 catalyst,

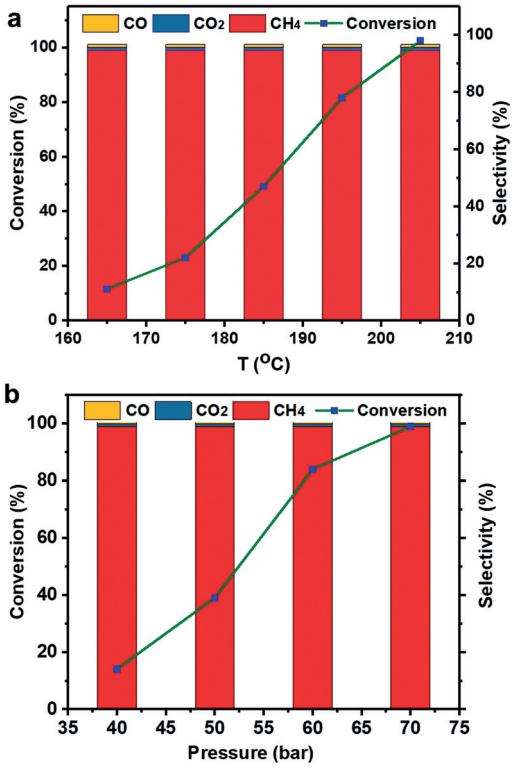

Figure 3. Influence of the reaction conditions on the reaction: a) 0.5 mmol substrate, 0.3 mol% of Ru, 0.5 mL solvent, 70 bar H_2, 20 h; b) 0.5 mmol substrate, 0.3 mol% of Ru, 0.5 mL solvent, 205 °C, 20 h.

efficiently undergoing conversion to 2-(methylamino)ethanol (**2b**) and methane in 69% and 97% yields, respectively (Table S4, entry 1). Urea (**1c**) was also investigated, with methane obtained in 41% yield and 99% selectivity at a slightly lower temperature of 180 °C. Under the applied conditions, the urea decomposes to afford fulminic acid.[46] Notably, direct hydrogenation of **2b** using Ru/SION-105 catalyst under the same conditions did not afford any methane or CO (Table S4, entry 3). This indicates that the cyclic carbamate intermediate is essential for the production of methane.

In conclusion, we described an indirect and sustainable CO_2 methanation route employing amino alcohols as relay molecules. The transformation was achieved using a catalyst comprising Ru NPs supported on a MOF (Ru/SION-105), with the benefits of the MOF support material demonstrated. Due to the small particle size and narrow size distribution of Ru NPs, the Ru/SION-105 catalyst is highly active for the reaction. Since oxazolidinones are easily prepared from the reaction of amino alcohols and CO_2, they are superior to other classes of relay molecules, that is, those based on diols or amines. This work paves the way towards the discovery of new efficient catalysts for the methanation of CO_2.

Acknowledgements

We thank the EPFL, Swiss National Science Foundation and the Swiss Competence Center for Energy Research (SCCER) for Heat and Electricity Storage for financial support. We also thank Pierre Mettraux and Lagrange Thomas for analytical support.

Conflict of interest

The authors declare no conflict of interest.

Keywords: CO_2 chemistry · green chemistry · metal–organic frameworks · sustainable chemistry

[1] W. C. Chen, J. S. Shen, T. Jurca, C. J. Peng, Y. H. Lin, Y. P. Wang, W. C. Shih, G. P. A. Yap, T. G. Ong, *Angew. Chem. Int. Ed.* **2015**, *54*, 15207 – 15212; *Angew. Chem.* **2015**, *127*, 15422 – 15427.
[2] S. Bontemps, *Coord. Chem. Rev.* **2016**, *308*, 117 – 130.
[3] M. Aresta, A. Dibenedetto, A. Angelini, *Chem. Rev.* **2014**, *114*, 1709 – 1742.
[4] P. Gao, S. G. Li, X. N. Bu, S. S. Dang, Z. Y. Liu, H. Wang, L. S. Zhong, M. H. Qiu, C. G. Yang, J. Cai, W. Wei, Y. H. Sun, *Nat. Chem.* **2017**, *9*, 1019 – 1024.
[5] W. Zhou, K. Cheng, J. C. Kang, C. Zhou, V. Subramanian, Q. H. Zhang, Y. Wang, *Chem. Soc. Rev.* **2019**, *48*, 3193 – 3228.
[6] X. P. Guo, Z. J. Peng, A. Traitangwong, G. Wang, H. Y. Xu, V. Meeyoo, C. S. Li, S. J. Zhang, *Green Chem.* **2018**, *20*, 4932 – 4945.
[7] C. S. Budi, H. C. Wu, C. S. Chen, D. Saikia, H. M. Kao, *ChemSusChem* **2016**, *9*, 2326 – 2331.
[8] J. N. Park, E. W. McFarland, *J. Catal.* **2009**, *266*, 92 – 97.
[9] T. Sakpal, L. Lefferts, *J. Catal.* **2018**, *367*, 171 – 180.
[10] W. D. Shafer, G. Jacobs, U. M. Graham, H. H. Hamdeh, B. H. Davis, *J. Catal.* **2019**, *369*, 239 – 248.
[11] Y. Yan, Q. J. Wang, C. Y. Jiang, Y. Yao, D. Lu, J. W. Zheng, Y. H. Dai, H. M. Wang, Y. H. Yang, *J. Catal.* **2018**, *367*, 194 – 205.
[12] X. Su, J. H. Xu, B. L. Liang, H. M. Duan, B. L. Hou, Y. Q. Huang, *J. Energy Chem.* **2016**, *25*, 553 – 565.
[13] F. Wang, S. He, H. Chen, B. Wang, L. R. Zheng, M. Wei, D. G. Evans, X. Duan, *J. Am. Chem. Soc.* **2016**, *138*, 6298 – 6305.
[14] W. T. Lee, A. P. van Muyden, F. D. Bobbink, Z. J. Huang, P. J. Dyson, *Angew. Chem. Int. Ed.* **2019**, *58*, 557 – 560; *Angew. Chem.* **2019**, *131*, 567 – 570.
[15] F. D. Bobbink, W. Gruszka, M. Hulla, S. Das, P. J. Dyson, *Chem. Commun.* **2016**, *52*, 10787 – 10790.
[16] P. D. Vaidya, E. Y. Kenig, *Chem. Eng. Technol.* **2007**, *30*, 1467 – 1474.
[17] X. G. Wang, W. Conway, D. Fernandes, G. Lawrance, R. Burns, G. Puxty, M. Maeder, *J. Phys. Chem. A* **2011**, *115*, 6405 – 6412.
[18] G. T. Rochelle, *Science* **2009**, *325*, 1652 – 1654.
[19] J. R. Khusnutdinova, J. A. Garg, D. Milstein, *ACS Catal.* **2015**, *5*, 2416 – 2422.
[20] R. Juárez, P. Concepción, A. Corma, H. García, *Chem. Commun.* **2010**, *46*, 4181 – 4183.
[21] M. Tamura, M. Honda, K. Noro, Y. Nakagawa, K. Tomishige, *J. Catal.* **2013**, *305*, 191 – 203.
[22] T. Niemi, I. Fernandez, B. Steadman, J. K. Mannisto, T. Repo, *Chem. Commun.* **2018**, *54*, 3166 – 3169.
[23] J. Paz, C. Perez-Balado, B. Iglesias, L. Munoz, *J. Org. Chem.* **2010**, *75*, 3037 – 3046.
[24] S. W. Foo, Y. Takada, Y. Yamazaki, S. Saito, *Tetrahedron Lett.* **2013**, *54*, 4717 – 4720.

[25] P. Hu, J. V. Morabito, C. K. Tsung, *ACS Catal.* **2014**, *4*, 4409 – 4419.
[26] Q. H. Yang, Q. Xu, S. H. Yu, H. L. Jiang, *Angew. Chem. Int. Ed.* **2016**, *55*, 3685 – 3689; *Angew. Chem.* **2016**, *128*, 3749 – 3753.
[27] M. T. Zhao, K. Yuan, Y. Wang, G. D. Li, J. Guo, L. Gu, W. P. Hu, H. J. Zhao, Z. Y. Tang, *Nature* **2016**, *539*, 76 – 80.
[28] X. L. Li, B. Y. Zhang, L. L. Tang, T. W. Goh, S. Y. Qi, A. Volkov, Y. C. Pei, Z. Y. Qi, C. K. Tsung, L. Stanley, W. Y. Huang, *Angew. Chem. Int. Ed.* **2017**, *56*, 16371 – 16375; *Angew. Chem.* **2017**, *129*, 16589 – 16593.
[29] Q. H. Yang, Q. Xu, H. L. Jiang, *Chem. Soc. Rev.* **2017**, *46*, 4774 – 4808.
[30] J. Zhu, P. M. Usov, W. Q. Xu, P. J. Celis-Salazar, S. Y. Lin, M. C. Kessinger, C. Landaverde-Alvarado, M. Cai, A. M. May, C. Slebodnick, D. R. Zhu, S. D. Senanayake, A. J. Morris, *J. Am. Chem. Soc.* **2018**, *140*, 993 – 1003.
[31] M. L. Ding, R. W. Flaig, H. L. Jiang, O. M. Yaghi, *Chem. Soc. Rev.* **2019**, *48*, 2783 – 2828.
[32] S. Shyshkanov, T. N. Nguyen, F. M. Ebrahim, K. C. Stylianou, P. J. Dyson, *Angew. Chem. Int. Ed.* **2019**, *58*, 5371 – 5375; *Angew. Chem.* **2019**, *131*, 5425 – 5429.
[33] H. Xu, B. Zhai, C. S. Cao, B. Zhao, *Inorg. Chem.* **2016**, *55*, 9671 – 9676.
[34] Y. Fang, J. L. Li, T. Togo, F. Y. Jin, Z. F. Xiao, L. J. Liu, H. Drake, X. Z. Lian, H. C. Zhou, *Chem* **2018**, *4*, 555 – 563.
[35] L. Q. Wu, J. L. Song, B. W. Zhou, T. B. Wu, T. Jiang, B. X. Han, *Chem. Asian J.* **2016**, *11*, 2792 – 2796.
[36] Z. H. Li, T. M. Rayder, L. S. Luo, J. A. Byers, C. K. Tsung, *J. Am. Chem. Soc.* **2018**, *140*, 8082 – 8085.
[37] L. S. Luo, W. S. Lo, X. M. Si, H. L. Li, Y. C. Wu, Y. Y. An, Q. L. Zhu, L. Y. Chou, T. Li, C. K. Tsung, *J. Am. Chem. Soc.* **2019**, *141*, 20365 – 20370.
[38] L. M. Ning, S. Y. Liao, H. G. Cui, L. H. Yu, X. L. Tong, *ACS Sustainable Chem. Eng.* **2018**, *6*, 135 – 142.
[39] V. B. Saptal, T. Sasaki, B. M. Bhanage, *ChemCatChem* **2018**, *10*, 2593 – 2600.
[40] H. Z. Bi, X. H. Tan, R. F. Dou, Y. Pei, M. H. Qiao, B. Sun, B. N. Zong, *Green Chem.* **2016**, *18*, 2216 – 2221.
[41] A. K. Das, R. S. Vemuri, I. Kutnyakov, B. P. McGrail, R. K. Motkuri, *Sci. Rep.* **2016**, *6*, 28050 – 28056.
[42] M. Atanassova, V. Kurteva, I. Billard, *Anal. Sci.* **2015**, *31*, 917 – 922.
[43] R. M. R. Dumpala, A. Boda, P. Kumar, N. Rawat, S. M. Ali, *Inorg. Chem.* **2019**, *58*, 11180 – 11194.
[44] M. J. Taylor, L. J. Durndell, M. A. Isaacs, C. M. A. Parlett, K. Wilson, A. F. Lee, G. Kyriakou, *Appl. Catal. B* **2016**, *180*, 580 – 585.
[45] X. H. Yang, X. M. Xiang, H. M. Chen, H. Y. Zheng, Y. W. Li, Y. L. Zhu, *ChemCatChem* **2017**, *9*, 3023 – 3030.
[46] E. Urbańczyk, M. Sowa, W. Simka, *J. Appl. Electrochem.* **2016**, *46*, 1011 – 1029.

Manuscript received: March 30, 2020
Revised manuscript received: May 28, 2020
Accepted manuscript online: June 9, 2020
Version of record online: July 10, 2020

